INTL JOURNAL OF ELECTRONICS AND TELECOMMUNICATIONS, 2026, VOL. 72, NO. 3, PP. 1-11
Manuscript received November 05, 2025; revised June, 2026. doi: 10.24425/ijet.2026.1718

Development of a ROS bridge communication framework for real-time water quality monitoring in Aquaculture Floating Net Cages

Bhakti Yudho Suprapto, Ilham Pratama, Muhammad Rafian Azim, and Suci Dwijayanti

***Abstract*—Conventional floating net cages (KJA), widely used in aquaculture, generally lack integrated water quality sensors and real-time monitoring systems, resulting in inadequate water quality management and undetected causes of fish mortality. This study addresses this gap by equipping KJA with sensors that continuously monitor key water quality parameters, temperature, pH, and dissolved oxygen, and transmit data directly to a centralized server for real-time analysis and visualization via a web-based platform. To achieve fast and reliable wireless communication between the buoy and net cage, the TCP/IP protocol is implemented within the Robot Operating System (ROS) framework. This enables seamless interfacing of non-ROS devices, such as ESP32 microcontrollers, with the ROS system hosted on a laptop, facilitating rapid and stable data transfer. System performance tests under varying network conditions, server loads, and user access showed average data transmission delays of approximately 1 second, with maximum delays ranging from 4 to 9 seconds. Additional TCP/IP communication tests revealed an average packet delivery latency of just 11 milliseconds, demonstrating the high efficiency of the wireless link. User experience evaluation found that 90% of participants rated the web interface as both easy to use and informative, receiving an overall "excellent" usability score. These findings confirm that the developed system significantly improves the effectiveness of real-time water quality monitoring in KJA operations, potentially reducing fish mortality caused by water quality issues.**

***Keywords*—floating net cages, monitoring system, real-time, sensors, water quality, web**

I. Introduction

NOWADAYS, the need for fish in the world is increasing, along with the awareness of the benefits of consuming fish for health and nutrition[1]. The increasing demand for fish, driven by population growth and changes in food preferences, has significantly advanced aquaculture. In freshwater fisheries cultivation, there are 3 methods to increase the income of farmers, namely floating net cages (KJA), bottom net cages (KJD), and fixed net cages (KJT)[2][3]. Among the three aquaculture methods, floating net cages have emerged as a widely adopted system due to their cost-effectiveness, flexibility, and suitability for use in natural waters. This method allows for high-density fish farming while utilizing the existing aquatic environment. Sustainable solutions, such as floating net cages, are crucial to the massive increase in aquaculture production that is required to fulfil the predicted demand for fish protein by 2030[4]. The KJA system is widely used because it can produce large amounts of fish. Floating net cages are one of the innovations commonly used in fish farming in open waters. This method is the most productive fish farming technique, and a method preferred by some people because it simplifies the sorting and harvesting process[5]. Important factors that must be considered in KJA cultivation are water quality and the selection of a suitable location for fish growth.

Conventional KJA has weaknesses related to several factors, especially regarding water quality management. Several previous studies have noted that floating net cages can contribute to local water pollution and put pressure on aquatic ecosystems. Example in reservoir, although parameters such as temperature, pH, and dissolved oxygen (DO) were still within acceptable ranges, ammonia levels were recorded as quite high near the floating net cage cultivation area[6]. This indicates a potential threat to fish health and water sustainability. In addition, floating net cages, which are open, can make them vulnerable to fluctuations in environmental conditions, such as temperature and dissolved oxygen levels, which will directly affect fish metabolism, growth rate, and survival. In addition, poor water quality conditions can inhibit fish growth, make them susceptible to attack by bacteria and parasites, and can even cause death[6]. Normal temperatures are also needed for fish growth and survival. The role of Dissolved Oxygen (DO) is very important in aquatic ecosystems because it affects the metabolism and respiration processes. Therefore, a KJA is needed that moves automatically based on the environment and is integrated with the monitoring display on the KJA and buoy. To obtain good results, floating net cages cannot be placed anywhere; for this reason, direct monitoring of the hydrographic conditions used in marine animal cultivation activities in floating net cages is needed.

To address these issues, research has increasingly focused on water quality monitoring, particularly the assessment of factors such as pH, temperature, and dissolved oxygen (DO). These factors are important measures of water health and directly affect fish welfare. The integration of sensor technology with microcontrollers and data-logging systems is a major milestone, providing continuous, real-time water-quality data. Among communication technologies, the Long Range (LoRa) protocol presents significant advantages, including wide-area coverage

This work was supported by the Directorate of Research, Technology, and Communication Service, The Directorate General of Higher Education, Research, and Technology (Research Contract No. 090/E5/PG.02.00.PL/2024).

Authors are with the Department of Electrical Engineering, Faculty of Engineering, Universitas Sriwijaya, Indonesia (e-mail: bhakti@ft.unsri.ac.id, sucidwijayanti@ft.unsri.ac.id, rafianazim6@gmail.com, ilhampratama11nya@gmail.com)

capability, low power consumption, and robust signal penetration in aquatic or semi-aquatic environments, making it optimal for remote KJA deployments. Previous studies have demonstrated IoT-enabled water quality monitoring frameworks employing web-based dashboards, machine learning analytics, and edge computing for remote status visualization and predictive management of aquaculture ponds and offshore cages. This research proposes the design and deployment of a LoRa-based IoT system incorporating movable buoys equipped with multi-point water quality sensors distributed over a defined spatial grid within KJA units to capture heterogeneous hydrographic dynamics. Data transmission leverages TCP/IP stack integration with robotic operating systems (ROS) for real-time data processing, fusion, and dissemination through responsive web applications, thereby enabling remote supervisory control and timely intervention against adverse water quality events. Research on web-based and remote monitoring systems has been conducted by researchers, including monitoring the quality of shrimp farming in ponds[7], pond water quality with IoT sensors and machine learning to predict the survival of fish species[8], monitoring water quality based on a web server using the MCU node ESP8266 module[9], monitoring water quality in offshore aquaculture cages based on Artificial Intelligence[10][11]. Water Quality Monitoring (WQM) is a cost-effective and efficient system designed to monitor drinking water quality, which makes use of Internet of Things (IoT) technology[8][12][13][14]. This web-based and IoT monitoring system is also used for other applications, such as heart rate and body temperature[15], air quality[16][17], and flood height[18].

In this study, a floating net cage system is designed that can be moved and uses a buoy placed about 20 meters as a sensor to determine the best water quality, so it requires multiple points. This is a challenge that must be solved. This study will employ the TCP/IP protocol and platforms like the Robot Operating System to facilitate remote data collecting, processing, and display via web applications[19][20][21][22]. This method enables aquaculture operators to remotely monitor water quality parameters, including pH, temperature, and dissolved oxygen, in real-time, thereby permitting prompt intervention to prevent fish mortality.

II. Autonomous Floating Net Cages System

Floating Net Cages (KJA) are cages equipped with nets used as a tool for fish farming activities. The floating net cage shape is rectangular with varying sizes, designed to be used on the surface of the water, and has nets on the sides to accommodate the fish being farmed[6].

Floating Net Cages (KJA) are one method of fish farming that utilizes existing water resources. KJA uses a light steel frame, and the floats are made of High-Density Polyethylene (HDPE). This cage is widely used because it is the right method for cultivating fish, where the fish can be monitored and are easier to feed. However, if the ratio of fish and the area of the cage is not appropriate and the environment is polluted, this cage becomes ineffective. This causes many fish to die. Therefore, the cage will be moved if the water quality is not good. So, it requires a driver in the cage. The success of implementing KJA is highly dependent on selecting the right location. In the development of this floating net cage, a floating net cage that can move automatically was created, based on location considerations that include water quality evaluation. This system is equipped with autonomous floats and various sensors used as references in the control system. In this study, the floating net cage system consists of one floating net cage as a control center and 4 floats located on the side of the floating net cage with a distance of approximately 20 meters, as in Fig. 1 below:

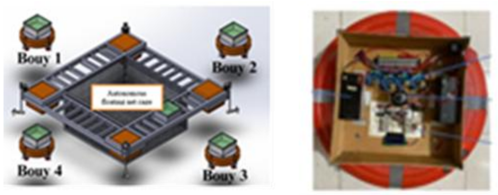

Fig.1. a) Configuration of the autonomous floating net cage system, b) The autonomous buoy

The autonomous floating net cage system can be seen in Fig. 1. This system has 4 floats that will help to observe the hydrographic conditions around the floating net cage. Each float has been equipped with various sensors, such as pH, temperature, and dissolved oxygen (DO), whose data will later be sent to the microcontroller on the floating net cage for further processing. The float, as seen in Fig. 2, is a float that can move automatically without user or operator intervention by using a DC motor as an actuator and sensors as microcontroller input.

III. Data Communication System

In running its operations, communication is required on the floating net cages and buoys. The communication carried out is the communication of sending and receiving data obtained from sensors on the floating net cages and buoys. On each floating net cage and buoy, 3 types of sensors affect water quality, namely temperature, pH, and dissolved oxygen (DO). If the sensor readings on the floating net cage for these three parameters are bad, which proves that the water quality in the floating net cage is bad, then the monitoring system will read on each sensor on the buoy. This is what causes problems with data communication in this floating net cage system. This section will discuss TCP/IP IP-based communication, multipoint-to-point topology, and LoRa technology in data communication systems. One of the most widely used communication protocols today is TCP/IP (Transmission Control Protocol/Internet Protocol). This protocol is a set of standard rules that allow devices in a network to communicate with each other. The TCP/IP architecture consists of four main layers, namely the Application Layer, Transport Layer, Internet Layer, and Network Access Layer. Each layer has a specific function in the communication process, from providing application services to physically sending data through the network media. In the context of a distributed control system or monitoring system, TCP/IP-based communication provides high flexibility in device integration, interoperability between platforms, and network scalability, making it very suitable for use in Internet of Things (IoT) and Industry 4.0-based systems. In the context of TCP communication, data transmission is done reliably using the principle of sequencing and acknowledgment. The number of bits sent in a unit of time can be calculated using the data rate equation :

$$R = \frac{L}{T} \quad (1)$$

where R is the data transmission rate (bps), L is the data length (bits), and T is the transmission time (seconds). Multipoint-to-point network topology is widely applied in monitoring or data acquisition systems. One of the basic probability formulas for collision in a multipoint system is:

$$P_c = 1 - \left(1 - \frac{1}{n}\right)^{\wedge} k \quad (2)$$

With Pc being the probability of a collision occurring, n the number of nodes, and k the number of nodes active at any one time. Besides communication protocols, network architecture significantly influences the efficiency and effectiveness of data transfer. A prevalent topology utilized in IoT systems and sensor networks is multipoint-to-point. In this design, many transmitting nodes (multipoint) transmit data to a central receiving node (point). This framework is extensively utilized in monitoring or data-collecting systems, where information from multiple remote sensors is aggregated centrally for subsequent analysis. The multipoint-to-point architecture offers advantages in resource efficiency and ease in data administration. The system can be configured to be more compact and energy-efficient by utilizing a central point as an information collector, particularly when integrated with low-power wireless communication technologies. LoRa is a wireless communication technology with a wide range and low power consumption. The basic equation that describes the relationship between the physical parameters of the LoRa signal is:

$$Data\ Rate\ (bps) = \frac{(Spreading\ Factor\ x\ Bandwidth)}{2^{\wedge}Spreading\ Factor} \quad (3)$$

LoRa (Long Range Radio) is a widely utilized wireless technology in multipoint-to-point applications. LoRa is a wireless communication system that emphasizes extensive range and low power usage. This technology employs chirp spread spectrum modulation and functions at ISM frequencies, including 433 MHz, 868 MHz, and 915 MHz. LoRa facilitates data transfer over distances of 10–15 km in unobstructed environments, rendering it suitable for applications necessitating long-range communication with comparatively low data rates. In the LoRa network design, data from several sensor devices is transmitted to one or more gateways, which subsequently relay the data to a central server through the internet or a local network. The integration of LoRa with a multipoint-to-point topology offers an exceptionally effective solution for many applications, including environmental monitoring, smart agricultural systems, smart cities, and extensive asset tracking, as seen in Fig. 2.

Fig.2. LoRa Technology

Integrating the TCP/IP protocol, multipoint-to-point topology, and LoRa technology enhances the reliability, efficiency, and power efficiency of data communication systems. These three components synergistically enhance the deployment of distributed communication systems tailored to the requirements of diverse sectors, ranging from industrial to public applications. Consequently, comprehending and executing the three elements are crucial in the development of a contemporary communication system that addresses current issues and requirements.

IV. METHOD

This research was conducted in a large water area and aims to determine water quality. The pH, DO, and temperature sensors affect water quality monitoring results. For data to be displayed on the website in real-time, PHP is used to create displays and receive data from sensors and store the data in MySQL. Floating net cages will move based on hydrographic condition data sent by the buoy, to determine the best position of the floating net cage a decision-making algorithm is created, this algorithm will determine the best water quality from the hydrographic data sent by the buoy and then maintain that position. If the hydrographic conditions in the floating net cage are good, the system will maintain its position. Conversely, suppose the hydrographic conditions around the floating net cage are bad. In that case, the floating net cage will run a decision-making algorithm to determine new coordinate points based on buoys that have the best hydrographic conditions. In monitoring the position of KJA and the buoy, a GPS Sensor Ublox is needed. A GPS Sensor can receive information from satellites in the form of data such as longitude and latitude. ESP32 reads the GPS sensor and then sends all data using wireless communication via ROS Bridge. ROS Bridge was chosen because this communication method offers a wide communication range and fast delivery. Furthermore, the data is sent to the ESP32 ROS Bridge, which will send it to the ESP32 web via LORA 02 RA. In sending sensor data to the monitoring website, the ESP32 web needs to be connected to the internet. The use of a modem in this study is useful for providing internet connection access and then spreading the network so that it can be captured by the ESP32. After sending the website created with PHP, which is integrated with MySQL. The data is received by the website to then be inserted into the database and then displayed on the KJA and buoy monitoring website, as seen in Fig. 3.

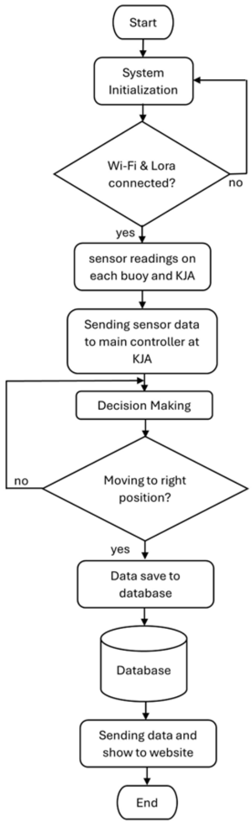

Fig. 3. Flowchart of the Data Communication

Fig. 4 is an IoT architecture based on Long Range. in the left part of the diagram, each buoy will send all information, including hydrographic data and position, to the automatic floating net cage using the LoRa-02 module. After the data is received, the ESP32 floating net cage on the KJA will upload data to the internet using the help of the GSM900A module, and the data uploaded by the KJA automatically includes all information on the buoy and the KJA itself.

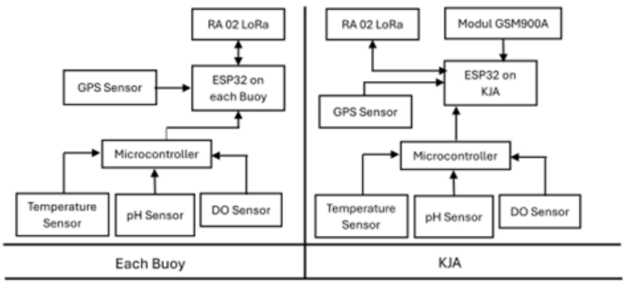

Fig. 4. Long Range Based IoT Architecture

A. Data collection

The data used in this study are primary in the form of pH values, temperature, dissolved oxygen content, position coordinates (buoy and KJA), and LoRa performance in communicating on the automatic floating net cage system; these data include RSSI, SNR, delay, and packet loss.

Before the sensor is used for data collection, calibration is performed on each sensor. Calibration of pH and temperature sensors using the help of a digital pH meter and a digital thermometer as a reference (true value), then the error value of each sensor will be calculated.

$$true\ value - sensor\ value = error \quad (4)$$

To calibrate the DO sensor, a table of temperature changes in dissolved oxygen concentration is used. The Table I used in the calibration process is based on the datasheet issued by the sensor brand.

TABLE I
DO LEVEL CHANGES AGAINST TEMPERATURE

T(^{0}C)	DO (mg/L)	T(^{0}C)	DO (mg/L)	T(^{0}C)	DO (mg/L)
0	14.60	16	9.86	32	7.30
1	14.22	17	9.64	33	7.17
2	13.80	18	9.47	34	7.06
3	13.44	19	9.27	35	6.94
4	13.08	20	9.09	36	6.84
5	12.76	21	8.91	37	6.72
6	12.44	22	8.74	38	6.60
7	12.11	23	8.57	39	6.52
8	11.83	24	8.41	40	6.40
9	11.56	25	8.25	41	6.33
10	11.29	26	8.11	42	6.23
11	11.04	27	7.96	43	6.13
12	10.76	28	7.83	44	6.06
13	10.54	29	7.68	45	5.97
14	10.31	30	7.56	46	5.88
15	10.06	31	7.43	47	5.79

The position of the buoy and KJA will be presented in the form of latitude and longitude coordinates. The latitude and longitude values are obtained from direct readings from the GPS sensor by extracting the National Marine Electronics Association (NMEA) code.

B. Data Performance of Long Range (LoRa)

The first performance parameter is the Received Signal Strength Indicator (RSSI). RSSI is a measure used to determine the quality of signal reception obtained. RSSI is measured on the receiver side while communicating with the sender. Table II is a grouping of RSSI values.

TABLE II
RSSI LEVEL STANDARD

RSSI Level	Description
> -70 dBm	Very Strong
-70 dBm s/d -86 dBm	Very Good
-86 dBm s/d -100 dBm	Good
-101 dBm s/d -110 dBm	Bad, Needs Improvement
< -110 dBm	Very Bad, Connection Failed

The second parameter is to signal-to-noise ratio (SNR), which is the ratio between the desired signal power and the noise power. This SNR is used as a standard measure of signal quality for communication systems. Table III shows the grouping of SNR values.

TABLE III
SNR LEVEL STANDARD

SNR Level	Description
29 dB >	Very Strong
20 dB – 29 dB	Very Good
11 dB – 20 dB	Good
7 dB – 10 dB	Bad
0 dB – 7dB	Very Bad

The next parameter is Delay, which is the length of time from the packet arrival to the packet completion transmission. The delay is calculated using the equation below.

$$delay = data\ entry\ time\ now - data\ time\ before \quad (5)$$

Delay has a benchmark value that is used to determine the category of delay value obtained. The delay value category is shown in Table IV.

TABLE IV
NETWORK QUALITY BASED ON DELAY

Delay (ms)	Category
< 150	Very Good
150 s/d 300	GodBagus
300 s/d 450	Normal
> 450	Bad

The last parameter is Packet loss, which is a condition when the sent packet fails to reach its destination. To calculate the percentage of packet loss in a transmission, use the formula below.

$$packet\ loss = \frac{Data\ sent - data\ received}{Data\ sent} \qquad (6)$$

Packet loss has a benchmark value that is used to determine the category of the loss value obtained. The value categories are shown in Table V.

TABLE V
NETWORK QUALITY BASED ON PACKET LOSS

Delay (ms)	Category
< 150	Very Good
150 s/d 300	Good
300 s/d 450	Normal
> 450	Bad

C. System Testing

After completing the design stage, the next step is to test the monitoring system on the floating net cages. The main purpose of this test is to evaluate the success and identify potential errors that may occur in the system that has been created. The testing process involves placing floating net cages in inland waters. During the test, the cages will take water quality readings using temperature sensors, pH sensors, and DO sensors. The data generated will be presented in real-time via the website. In addition, the test also includes a usability test of the website. By involving elements such as time delay between monitoring tools and devices and usability tests. The interval class of usability assessment criteria can be seen in Table VI.

TABLE VI
NETWORK QUALITY BASED ON PACKET LOSS

Quadrant	Interval Class	Assessment Criteria
V	4,21-5,00	Very Good
IV	3,41-4,20	Good
III	2,61-2,40	Good Enough
II	1,81-2,60	Bad
I	1,00-1,80	Very Bad

This test is expected to provide a comprehensive picture of the performance and reliability of the monitoring system that has been designed, and evaluate the success, including finding the minimum time delay and getting the highest score regarding the level of user convenience based on the questionnaire created.

V. RESULT AND DISCUSSION

This section discusses the results of the communication system design between autonomous buoys and autonomous KJA to transmit sensor data, coordinate positions, and PWM (Pulse Width Modulation) data on the motors of each buoy and KJA. The tests carried out are in the form of LoRa communication tests and ROS bridge communication, use of ROS bridge communication, and display on the website.

This floating net cage system has 4 buoys and 1 floating net cage equipped with pH, temperature, and DO sensors on each buoy and KJA. Each buoy is placed on each side of the floating net cage: the right side, left side, front side, and back side, as in Fig. 1. After designing and making the tool, the KJA and buoy are obtained as shown in Fig. 5.

(a) (b)
Fig. 5. Design Results (a) KJA & (b) Buoy

A. LoRa Performance Testing Simulation

This test is carried out to see how reliable the performance of communication using LoRa is, the system is tested without using distance so that it can eliminate factors such as weak signals captured, this is done to help solve problems that occur in existing data communications, this test is in the form of peer to peer, Multi Point to Point, and Point to Multi Point.

B. Peer-to-peer test

This experiment tests Lora sending data in one direction and only to one node. The test is carried out twice, using delay and without delay, to see the packet loss and delay that occur during delivery.

C. Peer-to-peer without Delay Testing

In this test, LoRA is tested in real time using 1 node without adding delay to LoRa, then the data is stored using PLX-DAQ. LoRa is tested by sending string data with a numeric value that will continue to increase by 1; the value will be captured on the receiving side and then observed how much data is lost during transmission. RSSI and SNR values will be observed to support the analysis process during the data transmission process.

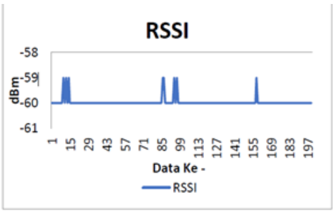

a)

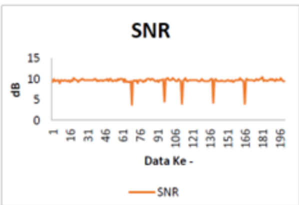

b)

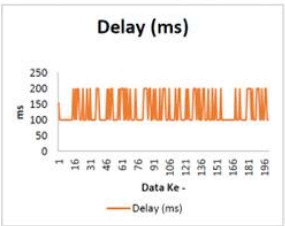

c)

Fig. 6. a) Lora 1 Node RSSI Graph Without Delay, b)LoRa 1 Node SNR Graph Without Delay, c) LoRa 1 Node Delay Graph Without Delay

In Fig. 6.a, the RSSI value of 200 data shows that the signal captured by the receiver is still classified as very good with an average RSSI value of -59.96 dBm. This is because testing between nodes is carried out without distance. Fig. 6.b shows the SNR value of 200 data shows that the received signal strength based on noise is at a poor index with an average SNR value of 10 dB, in some data there is a very low SNR value so that it enters the very poor index, however the data can still be received without experiencing data defects (corrupted data). Then Fig. 6.c. shows the delay value of 200 data with an average of 131 ms, in some data the delay value increases to 200 ms, this is due to packet loss, so that the next data received needs to wait for a longer pause.

TABLE VII
NETWORK QUALITY BASED ON PACKET LOSS

LoRa Node	RSSI	SNR	Delay (ms)	Data Id	Packet Loss
1	-60	9.5	100	1684	
1	-59	9.5	100	1685	1
1	-60	9.75	199	1687	
1	-60	9.25	100	1688	1
1	-60	9.75	199	1690	
1	-60	9.5	101	1691	1
1	-60	10.25	199	1693	1
1	-60	10	199	1695	

Packet loss that occurs during transmission is calculated by looking at the difference in id in the received data. Table VII is a sample of data from 200 data received; there is a jump in id data from 1685 to 1687. Based on this calculation, there should be 264 data received, but the data on the receiving side only gets 200 data, so there are 64 packet losses with a percentage of 32%. This results in packet loss on LoRa being in the bad index.

D. Peer-to-peer with Delay 100 ms Testing

In this test, LoRA is tested in real time using 1 node by adding a 100ms delay to LoRa, then the data is stored using PLX-DAQ. LoRa is tested by sending 200 strings of data with a numeric value that will continue to increase by 1, the value will be captured on the receiving side and then observed how much data is lost during transmission. RSSI and SNR values will be observed to support the analysis process during the data transmission process. The RSSI value of 200 data shows that the signal captured by the receiver is still classified as very good with an average RSSI value of -62.235 dBm. This is because testing between nodes is carried out without distance. The SNR value of 200 data shows that the received signal strength based on noise is at a poor index, with an average SNR value of 9.85 dB. In some data, there is a very low SNR value, so that it enters the very poor index, but the data can still be received without experiencing data defects (corrupted data). The delay value of 200 data with an average of 197 ms, the increase in the delay value occurs due to the addition of a 100 ms delay on the sender side, which aims to see the difference in packet loss when using delay.

Packet loss that occurs during delivery is calculated by looking at the difference in ID on the data received. Figure 14 and Table VIII are a sample of data from 200 data points received. It can be seen from the image that there is no packet loss during delivery, which occurs due to the addition of delay on the sender's side.

TABLE VIII
PACKET LOSS LORA 1 NODE WITH DELAY

No	Lora Node	RSSI	SNR	Delay (ms)	Data id	Pocket Loss
1	1	-59	9,75	196	232	0
2	1	-59	9,25	195	233	0
3	1	-59	9,75	198	234	0
4	1	-59	9,5	199	235	0
5	1	-59	9,75	201	236	0

E. LoRa Multi Point to Point Experiment

This test 1 LoRa receiving data from 5 other LoRa nodes, the test is carried out without delay to see the packet loss and delay that occurs in the delivery. Each node is run using a different frequency so that data collapse does not occur (overwritten) so that data transmission can be carried out continuously/spamming, to capture data at different frequencies, the receiving node changes the frequency found on each sending node, the frequency used is the default frequency of 433Mhz for node 1, 460Mhz for node 2, 470Mhz for node 3, 480Mhz for node 4, 490Mhz for node 5.

TABLE IX
MULTI-POINT TO POINT EXPERIMENT RESULTS (NODE 5)

No	Lora Node	RSSI	SNR	Delay (ms)	Data Id
56	4	-66	6.5	160	3421
57	3	-92	8.25	1748	1
58	4	-66	6.5	128	3425
59	2	-80	8.5	480	16757
60	4	-66	6.25	97	3428
61	1	-76	8.25	603	5
62	4	-66	6.5	191	3434
63	1	-66	9	201	12

Based on Table IX, the Multi Point to Point Experiment Results Table shows sample data received from the receiver side. In the received data, there were only 4 nodes' data that were successfully received. In the experiment, the data obtained on node 3 experienced congestion, and the data on node 3 could not be received properly, so a refresh was performed on the microcontroller, but this did not change the conditions on node 3. This condition can be seen in Table X.

TABLE X
MULTI POINT TO POINT EXPERIMENT RESULTS (NODE 3)

No	Lora Node	RSSI	SNR	Delay (ms)	Data Id
96	1	-65	9	32	38
97	4	-67	6.5	287	3521
98	1	-65	10	190	44
99	2	-80	9	319	16912
100	1	-57	9.25	254	52
101	3	-92	8	3496	1
102	4	-67	6	512	3537
103	2	-80	9.25	480	16936

F. LoRa Point to Multi Point Experiment

This experiment tests one LoRa sending data in one direction and tests with 5 receiver nodes, then examines the packet loss and delay that occurs in data transmission. This experiment uses the parse packet method to send data at once. The purpose of using this method is so that the sender node does not need to send with a queuing system, so that data can be received by each node simultaneously. Then the receiver node will parse the received packet, using parsing logic. Then enter the received value into the function that matches the receiver node address.

In Fig. 7, the RSSI value of 200 data on each node shows that the signal captured on the receiver side is classified as very good with an average RSSI value for node 1 -52 dBm, node 2 -52 dBm, node 3 -53 dBm, node 4 -54 dBm, node 5 -55 dBm. This is because testing between nodes is done without distance.

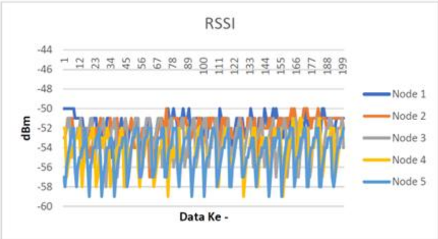

a)

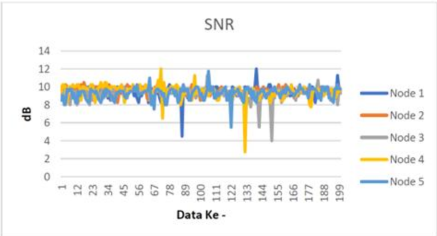

b)

Fig. 7. Five Node a) RSSI Value Graph, b)SNR Value Graph

The SNR value of 200 data shows that the received signal strength based on the noise ratio is at a poor index with an average SNR value for node 1 of 9.4 dB, node 2 of 9.5 dB, node 3 of 9.2 dB, node 4 of 9.4 dB, and node 5 of 9.3 dB. In some data, there is a very low SNR value, so it enters the very poor index. Due to excessive noise, some PWM data at several nodes are lost, or the received PWM value is incorrect.

The delay value of 200 data with an average of 197 ms. The increase in the delay value occurs due to the addition of a 100 ms delay on the sender’s side. The addition of a delay on the sender’s side aims to eliminate packet loss.

TABLE XI
THE PARAMETERS OF THE SENSOR

Lora Node	RSSI	SNR	PWM 01	PWM 02	PWM 03	PWM 04	PWM 05	Delay
1	-50	9.75	106	106	106	106	106	205
1	-50	9.75	107	107	107	107	107	204
1	-50	9.75	108	108	108	108	108	204
1	-50	9.5	109	109	109	109	109	195
1	-50	10	110	110	110	110	110	203
1	-50	9.5	111	111	111	111	111	205
1	-50	10	112	112	112	112	112	204
1	-50	9.75	113	113	113	113	113	194
1	-50	9.5	114	114	114	114	114	205
1	-50	10	115	115	115	115	115	204

Based on Table XI. The data received by node 1 does not experience packet loss; this is due to the addition of delay from the sender's side. Therefore, the use of LoRa for point-to-multipoint communication cannot be done because of the delay on the sender's side, which results in the slower movement of the buoy in the floating net cage system (KJA). So that the KJA system that moves based on the formation cannot function properly.

G. *Communication Testing Using Ros Bridge*

This experiment was conducted to see the reliability of the previously created ROS bridge communication; data collection was conducted at Kambang Iwak Kecik. This test is divided into communication at KJA, buoy 1, buoy 2, buoy 3, and buoy 4.

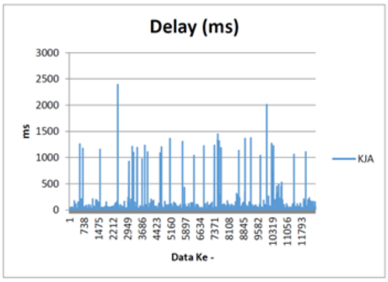

Fig. 8. KJA Input Node Delivery Delay Graph

TABLE XII
KJA COMMUNICATION QUALITY CALCULATION DATA – INPUT

Trial Period	04:13,980
Total Packet Loss	75340
Highest Delay (ms)	2394
Amount of Data Received	12518
The Amount of Data Should Be	87856
Percentage Packet Loss (%)	85,75
Average Delay (ms)	19

Based on Fig. 8 and Table XII, during the testing process, there is still a delay, but it is still understandable, and the master receives 12518 data with a span of 4 minutes 14 seconds, with the longest delay being 2394 milliseconds or 2.4 seconds, with an average delay of 19 milliseconds. The last data received during the experiment had a data id of 95454 while the first data had an id of 7598, by finding the amount of data and calculating the difference in data ids received, the packet loss that occurred during the experiment amounted to 75,340 data, so that the percentage of packet loss was at 85.7%, high packet loss is due to sleep rate/program execution pause on ROS. High packet loss causes the length of time the KJA positions the heading value to 0, resulting in a long KJA heading to the position it should occupy. despite communication disruptions during the KJA experiment, it can still complete its mission, namely, heading to the position it should.

TABLE XIII
KJA COMMUNICATION QUALITY CALCULATION DATA – OUTPUT

Total Packet Loss	0
Highest Delay (ms)	2406
Amount of Data Received	12518
The Amount of Data Should Be	12518
Persentase Packet Loss (%)	0
Delay Average (ms)	30

Based on Table XIII, the output node at KJA experiences a time delay that is almost the same as receiving data at ROS. This is due to the PWM output generated from ROS having to wait for input from the KJA input node. When ROS is run with a program execution pause, the PWM value issued by ROS follows the capabilities of esp32 at the output node, so packet loss on the output side can be avoided.

H. *Ros Bridge communication experiment on Buoy*

In Fig. 9 below, it can see the delay graph in the communication experiment during data transmission at the input node of buoy 1. Based on Fig. 9 and Table XIV. During the test process the master received 29403 data with a span of 5 minutes 53 seconds, with the longest delay being 1984 milliseconds or 1.9 seconds, with an average delay of 11 milliseconds. The last data received during the experiment has data id 260664 while the first data has id 117079, by finding the amount of data and calculating the difference in data id received, the packet loss that occurred during the experiment amounted to 114,183 data, so the percentage of packet loss was at 79.5%, high packet loss is due to sleep rate/program execution pause on ROS. High packet loss does not cause loss of direction on buoy 1, this is supported by the average delay that occurs on buoy 1 during transmission, only around 11 milliseconds.

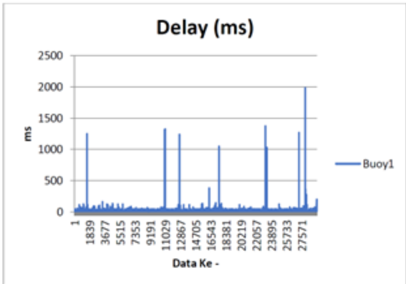

Fig. 9. Delay Graph of Buoy 1 Input Node Delivery

TABLE XIV
BUOY 1 COMMUNICATION QUALITY CALCULATION DATA – INPUT

TRIAL PERIOD	05:53,010
TOTAL PACKET LOSS	114183
HIGHEST DELAY (MS)	1984
AMOUNT OF DATA RECEIVED	29403
THE AMOUNT OF DATA SHOULD BE	143586
PERCENTAGE PACKET LOSS (%)	79,52
AVERAGE DELAY (MS)	11

TABLE XV
BUOY 1 COMMUNICATION QUALITY CALCULATION DATA – INPUT

Total Packet Loss	0
Highest Delay (ms)	1994
Amount of Data Received	29403
The Amount of Data Should Be	29403
Percentage Packet Loss (%)	0
Delay Average (ms)	21

Based on Table XV. The output node on buoy 1 experiences a time delay that is almost the same as receiving data on ROS, This is because the PWM output generated from ROS must wait for input from the input node of buoy 1. When ROS is run with a program execution pause, the PWM value issued by ROS follows the capabilities of the ESP32 on the output node, so that packet loss on the output side can be avoided.

I. *Ros Bridge communication experiment on Buoy 2*

The delay graph in the communication experiment when sending data at the input node of float 2 can be seen in Figure 10.

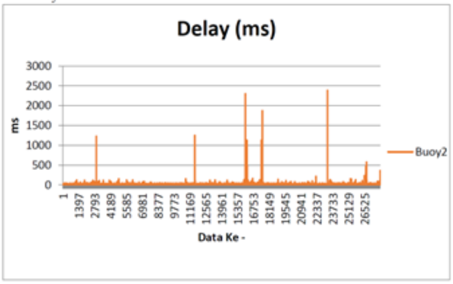

Fig. 10. Delay Graph of Buoy 2 Input Node Delivery

Based on Fig. 20 and Table XVI. During the testing process, the master received 27914 data with a time span of 5 minutes 52 seconds, with the longest delay at 2384 milliseconds or 2.3 seconds, with an average delay of 12 milliseconds. The last data received during the experiment has a data id of 96345 while the first data has an id of 128, by finding the number of data and calculating the difference in the data id received, the packet loss that occurred during the experiment was 68,303 data, so that the percentage of packet loss was at 71%, high packet loss was caused by the sleep rate/program execution pause on ROS. High packet loss did not cause loss of direction on buoy 2; this is supported by the average delay that occurred on buoy 2 during transmission of only around 12 milliseconds.

TABLE XVI
BUOY 2 COMMUNICATION QUALITY CALCULATION DATA – INPUT

Trial Period	05:52,690
Total Packet Loss	68305
Highest Delay (ms)	2384
Amount of Data Received	27914
The Amount of Data Should Be	96218
Percentage Packet Loss (%)	70,98
Average Delay (ms)	12

Based on Table XVII. The output node on buoy 2 experiences a time delay that is almost the same as the data reception on ROS. This is because the PWM output generated from ROS must wait for input from the input node of buoy 2. When ROS is run with a program execution pause, the PWM value issued by ROS follows the capabilities of the ESP32 on the output node, so that packet loss on the output side can be avoided.

TABLE XVII
BUOY 2 COMMUNICATION QUALITY CALCULATION DATA – OUTPUT

Total Packet Loss	0
Highest Delay (ms)	2393
Amount of Data Received	27914
The Amount of Data Should Be	27914
Percentage Packet Loss (%)	0
Delay Average (ms)	23

J. *Ros Bridge communication experiment on Buoy 3*

Delay during data transmission of input node buoy 3 during testing as seen in Fig. 11. Based on Fig. 11 and Table XVIII during the testing process, the master received 30245 data with a time span of 5 minutes 53 seconds, with the longest delay at 2012 milliseconds or 2 seconds, with an average delay of 11 milliseconds. The last data received during the experiment has a data id of 143271 while the first data has an id of 47893, by finding the number of data and calculating the difference in the received data id, the packet loss that occurred during the experiment was 65,134 data, so the percentage of packet loss was at 68%, high packet loss was caused by the sleep rate/program execution pause on ROS. High packet loss did not cause loss of direction on buoy 3; this is supported by the average delay that occurred on buoy 3 during transmission of only around 11 milliseconds.

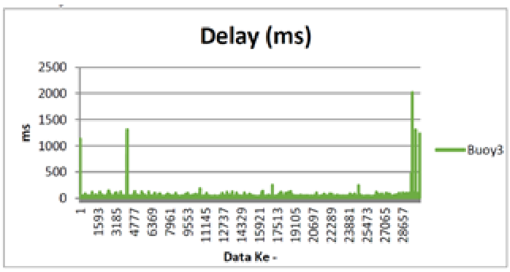

Fig. 11. Delay Graph of Buoy 3 Input Node Delivery

TABLE XVIII
BUOY 3 COMMUNICATION QUALITY CALCULATION DATA – INPUT

Trial Period	05:52,900
Total Packet Loss	65134
Highest Delay (ms)	2012
Amount of Data Received	30245
The Amount of Data Should Be	95379
Percentage Packet Loss (%)	68,2
Average Delay (ms)	11

TABLE XIX
BUOY 3 COMMUNICATION QUALITY CALCULATION DATA – OUTPUT

Total Packet Loss	0
Highest Delay (ms)	2023
Amount of Data Received	30245
The Amount of Data Should Be	30245
Percentage Packet Loss (%)	0
Delay Average (ms)	22

Table XIX show the output node on buoy 3 experiences a time delay that is almost the same as receiving data on ROS. This is because the PWM output generated from ROS must wait for input from the input node of buoy 3. When ROS is run with a program execution pause, the PWM value issued by ROS follows the capabilities of the ESP32 on the output node, so that packet loss on the output side can be avoided.

K. *Ros Bridge communication experiment on Buoy 4*

The delay during data transmission at the input node of buoy 4 during testing as seen in Fig. 12.

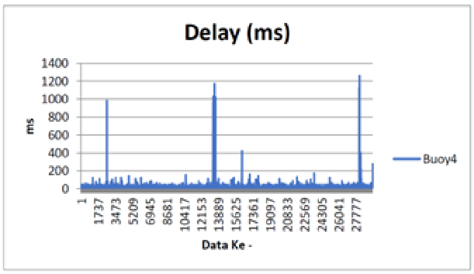

Fig. 12. Delay Graph of Buoy 4 Input Node Delivery

Based on Fig. 12 and Table XX, during the testing process, the master received 29,497 data points with a period of 5 minutes and 53 seconds, with the longest delay at 1,259 milliseconds (1.3 seconds), and an average delay of 11 milliseconds. The last data received during the experiment has a data id of 157961 while the first data has an id of 61474, by finding the number of data and calculating the difference in the received data id, the packet loss that occurred during the experiment was 66,991 data, so the percentage of packet loss was at 69%, high packet loss was caused by the sleep rate/program execution pause on ROS. High packet loss did not cause loss of direction on buoy 4, this is supported by the average delay that occurred on buoy 4 during transmission of only around 11 milliseconds.

TABLE XX
BUOY 4 COMMUNICATION QUALITY CALCULATION DATA – INPUT

Trial Period	05:52,850
Total Packet Loss	66991
Highest Delay (ms)	1259
Amount of Data Received	29497
The Amount of Data Should Be	96488
Percentage Packet Loss (%)	69,42
Average Delay (ms)	11

Table XXI gives information about the output node on buoy 4 experiences a time delay that is almost the same as the data reception on ROS This is because the PWM output generated from ROS must wait for input from the input node of buoy 4. When ROS is run with a program execution pause, the PWM value issued by ROS follows the capabilities of the ESP32 on the output node, so that packet loss on the output side can be avoided.

TABLE XXI
BUOY 4 COMMUNICATION QUALITY CALCULATION DATA – OUTPUT

Total Packet Loss	0
Highest Delay (ms)	1268
Amount of Data Received	29497
The Amount of Data Should Be	29497
Percentage Packet Loss (%)	0
Delay Average (ms)	22

L. *Sending data to the website*

On this website, there are several functions on this website, namely monitoring and sending data. For monitoring, users are presented with a summary of important information related to the condition of the Floating Net Cages and buoys. This display is designed to provide quick and easy access to data that is essential for the management and monitoring of fish farming systems. One of the main features is an interactive map that shows the position and movement of the cages and buoys. This map not only visualizes the location of the cages but also provides an overview of the distribution of buoys around them, allowing users to monitor operational dynamics in real time. The monitoring page can be seen on Fig. 13.

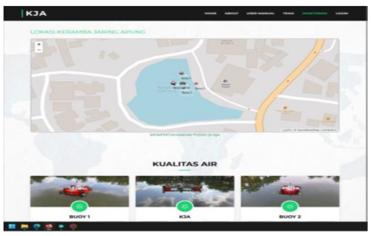

Fig. 13. Monitoring map view

Each buoy is equipped with sensors that collect crucial environmental data, such as water temperature, water pH, and DO sensors. This display includes images of the KJA and each buoy taking readings from the three main sensors. This display is made interactive so that users can click to see more detailed information. The sensor section monitoring page can be seen in Fig. 14.

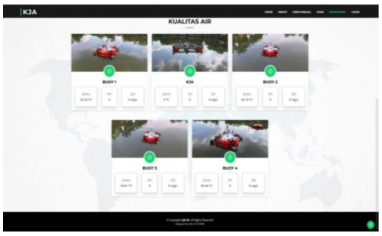

Fig. 14. Sensor monitoring display

On this page, users can view temperature, pH, and dissolved oxygen (DO) sensor values obtained from floating net cages (KJA) and all floats. This information is presented in real time to provide an accurate picture of water conditions. Users can monitor changes in temperature, acidity (pH), and dissolved oxygen levels at various locations, which are crucial for maintaining a healthy aquatic ecosystem and ensuring an optimal environment for aquatic life. This data is also useful for scientific analysis and decision-making in water resource management. Each floating net cage and float display has a detailed view that displays graphical data from the temperature, pH, and DO sensors. This data is crucial for monitoring environmental conditions in real time and ensuring that these parameters are within safe limits. With clear and detailed visualizations, users can easily see changes in these parameters over time. This allows for more in-depth analysis and better decision-making in maintaining water quality and ecosystem health. Furthermore, the graphical presentation of the data makes it easier for users to detect anomalies or drastic changes that may require immediate action, thereby increasing responsiveness and efficiency in environmental management. This test involves sending location and sensor data to a website using the same network. The data is sent via the IP address of a laptop displaying a local website. The purpose of this test is to monitor the delay in receiving data on the website. In this test, the website is tested in receiving data and displaying it in real-time to see the delay in delivery. This test is performed using a 4-buffer in sending location and sensor data to the website server; the delivery uses the website's domain that displays a website that can be accessed anywhere. The data collected by the website in the database will then be used to observe the delay in receiving data to the website. In the sensor section, the delay value from 17 data points, namely the ID, each sensor, and time, is obtained on average 1 second, and in some cases, the delay value increases to 7 seconds.

VI. CONCLUSION

This research confirms that LoRa communication is inadequate for real-time data transmission between the buoy and the KJA due to its inherent high packet loss rates and latency. Such limitations undermine timely sensor data acquisition required by robotic systems to execute precise PWM control on the microprocessor, leading to delayed actuator responses. Multipoint-to-point tests demonstrated that LoRa's transmission delay and packet loss prevent reliable real-time monitoring and control in aquaculture environments.

To overcome these challenges, a TCP/IP communication approach utilizing the ROS bridge was implemented. The ROS bridge facilitates efficient interfacing of non-ROS microcontrollers like ESP32 with the ROS environment, enabling rapid and reliable bidirectional data flow. Experimental evaluation showed that the ROS bridge reduced communication delay to an average of 10 milliseconds, enabling synchronous PWM signal generation critical for robotic operations. From a practical standpoint, these findings indicate that ROS-based TCP/IP communication is a robust solution for integrating fast sensor feedback in automated aquaculture systems, ensuring real-time responsiveness and enhancing operational reliability. This confirms the feasibility of deploying scalable remote monitoring platforms for KJA management, facilitating timely decision-making to maintain optimal water quality and reduce fish mortality.

REFERENCES

[1] R. Pramana, B. Y. Suprapto, and Z. Nawawi, "Application of fuzzy logic in decision-making process for relocation of floating net cages in river fish farming," *Glob. J. Environ. Sci. Manag.*, vol. 10, no. 1, pp. 117–132, 2024.

[2] H. Saksono and K. J. Utami, "Ekonomi Biru: Profil Kekayaan Laut dan Tingkat Kemiskinan di Wilayah Kepulauan Sulawesi Tenggara (2019-2023)," *Kainawa J. Pembang. dan Budaya*, vol. 6, no. 2, pp. 139–150, 2024.

[3] M. F. Arianto, "Potensi wilayah pesisir di negara Indonesia," *J. Geogr.*, vol. 10, no. 1, pp. 204–215, 2020.

[4] M. Arrazy and R. Primadini, "Potensi subsektor perikanan pada provinsi-provinsi di Indonesia," *J. Bina Bangsa Ekon.*, vol. 14, no. 1, pp. 1–13, 2021.

[5] I. Priyanto, C. A. Hartanto, and A. M. Arymurthy, "Change detection of floating net cages quantities utilizing faster R-CNN," in *2020 3rd International Conference on Computer and Informatics Engineering (IC2IE)*, IEEE, 2020, pp. 140–145.

[6] D. Arisanty, K. P. Hastuti, S. Adyatma, and M. Azhari, "The impact of floating net cages on the water quality of riam kanan reservoir, south kalimantan," in *IOP Conference Series: Earth and Environmental Science*, IOP Publishing, 2021, p. 12040.

[7] M. H. Haj, N. Zulbainarni, and N. Novindra, "Strategi dan kebijakan pengelolaan usaha budidaya lobster mutiara (P. ornatus) berkelanjutan di provinsi sulawesi selatan," *J. Kebijak. Perikan. Indones.*, vol. 15, no. 1, pp. 1–9, 2023.

[8] W. Hassan, M. Føre, H. A. Urke, T. Kristensen, J. B. Ulvund, and J. A. Alfredsen, "System for real-time positioning and monitoring of fish in commercial marine farms based on acoustic telemetry and internet of fish (iof)," in *ISOPE International Ocean and Polar Engineering Conference*, ISOPE, 2019, p. ISOPE-I.

[9] D. Hermanto, D. Stiawan, B. Y. Suprapto, E. Permata, and E. P. Widiyanto, "New Approach Monitoring System with ESP32 and MQTT for the Best Position of the Floating Net Cage," in *2023 10th International Conference on Electrical Engineering, Computer Science and Informatics (EECSI)*, IEEE, 2023, pp. 139–144.

[10] M. N. Asgher and M. T. Iqbal, "Development of a Low-Cost, Open-Source LoRA-based SCADA System for Remote Monitoring of a Hybrid Power System for an Offshore Aquaculture Site in Newfoundland," *Eur. J. Electr. Eng. Comput. Sci.*, vol. 7, no. 6, pp. 65–73, 2023.

[11] Y. Wei, Q. Wei, and D. An, "Intelligent monitoring and control technologies of open sea cage culture: A review," *Comput. Electron. Agric.*, vol. 169, no. July 2019, p. 105119, 2020, doi: 10.1016/j.compag.2019.105119.

[12] L. Parri, S. Parrino, G. Peruzzi, and A. Pozzebon, "Offshore LoRaWAN networking: Transmission performances analysis under different environmental conditions," *IEEE Trans. Instrum. Meas.*, vol. 70, pp. 1–10, 2020.

[13] G. Mageshkumar, S. P. Rao, S. Suthagar, K. Hemalatha, K. Gowtham, and T. Hariharan, "Design and Implementation of a Solar Powered Floating Device for Water Quality Monitoring in Inland Aquaculture Farms Using LoRa Wireless Communication," in *Inventive Computation*

and Information Technologies: Proceedings of ICICIT 2022, Springer, 2023, pp. 687–705.

[14] A. T. Demetillo, M. V Japitana, and E. B. Taboada, "A system for monitoring water quality in a large aquatic area using wireless sensor network technology," *Sustain. Environ. Res.*, vol. 29, no. 1, p. 12, 2019, doi: 10.1186/s42834-019-0009-4.

[15] M. F. Mazelam and S. A. Zulkifli, "IoT Based Health Monitoring for Heart Rate and Body Temperature," *Evol. Electr. Electron. Eng.*, vol. 4, no. 1, pp. 119–127, 2023.

[16] J. Jo, B. Jo, J. Kim, S. Kim, and W. Han, "Development of an IoT-based indoor air quality monitoring platform," *J. Sensors*, vol. 2020, no. 1, p. 8749764, 2020.

[17] K. D. Purkayastha, R. K. Mishra, A. Shil, and S. N. Pradhan, "IoT based design of air quality monitoring system web server for android platform," *Wirel. Pers. Commun.*, vol. 118, no. 4, pp. 2921–2940, 2021.

[18] M. I. Zakaria, W. A. Jabbar, and N. Sulaiman, "Development of a smart sensing unit for LoRaWAN-based IoT flood monitoring and warning system in catchment areas," *Internet Things Cyber-Physical Syst.*, vol. 3, pp. 249–261, 2023.

[19] T. Murkomen, "Performance, privacy, and security issues of TCP/IP at the application layer: A comprehensive survey," 2024.

[20] A. Kabanov and V. Kramar, "Marine internet of things platforms for interoperability of marine robotic agents: An overview of concepts and architectures," *J. Mar. Sci. Eng.*, vol. 10, no. 9, p. 1279, 2022.

[21] M. E. Söyünmez, "Browser-Based Lightweight Cross-Platform Web Control System for Autonomous Robots Operating With Ros," 2023, *İzmir Ekonomi Üniversitesi*.

[22] E. A. Shammar and A. T. Zahary, "The Internet of Things (IoT): a survey of techniques, operating systems, and trends," *Libr. Hi Tech*, vol. 38, no. 1, pp. 5–66, 2020.